Environmental Sciences Europe

RESEARCH

Open Access

Controlling blooms of *Planktothrix rubescens* by optimized metalimnetic water withdrawal: a modelling study on adaptive reservoir operation

Chenxi Mi[1,2*], David P. Hamilton[3], Marieke A. Frassl[3,4], Tom Shatwell[1], Xiangzhen Kong[1,5], Bertram Boehrer[1], Yiping Li[6], Jan Donner[7] and Karsten Rinke[1]

Abstract

Background: Aggregations of cyanobacteria in lakes and reservoirs are commonly associated with surface blooms, but may also occur in the metalimnion as subsurface or deep chlorophyll maxima. Metalimnetic cyanobacteria blooms are of great concern when potentially toxic species, such as *Planktothrix rubescens,* are involved. Metalimnetic blooms of *P. rubescens* have apparently increased in frequency and severity in recent years, so there is a strong need to identify reservoir management options to control it. We hypothesized that *P. rubescens* blooms in reservoirs can be suppressed using selective withdrawal to maximize its export from the reservoir. We also expect that altering the light climate can affect the dynamics of this species. We tested our hypothesis in Rappbode Reservoir (the largest drinking water reservoir in Germany) by establishing a series of withdrawal and light scenarios based on a calibrated water quality model (CE-QUAL-W2).

Results: The novel withdrawal strategy, in which water is withdrawn from a certain depth below the surface within the metalimnion instead of at a fixed elevation relative to the dam wall, significantly reduced *P. rubescens* biomass in the reservoir. According to the simulation results, we defined an optimal withdrawal volume to control *P. rubescens* blooms in the reservoir as approximately 10 million m^3 (10% of the reservoir volume) during its bloom phase. The results also illustrated that *P. rubescens* growth can be most effectively suppressed if the metalimnetic withdrawal is applied in the early stage of its rapid growth, i.e., before the bloom occurs. In addition, our study showed that *P. rubescens* biomass gradually decreased with increasing light extinction and nearly disappeared when the extinction coefficient exceeded 0.55 m^{-1}.

Conclusions: Our study indicates the rise in *P. rubescens* biomass can be effectively offset by selective withdrawal as well as by reducing light intensity beneath the water surface. Considering the widespread occurrence of *P. rubescens* in stratified lakes and reservoirs worldwide, we believe the results will be helpful for scientists and managers working on other water bodies to minimize the negative impacts of this harmful cyanobacteria. Our model may serve as a transferable tool to explore local dynamics in other standing waters.

*Correspondence: chenxi.mi@ufz.de

[1] Department of Lake Research, Helmholtz Centre for Environmental Research, Magdeburg, Germany
Full list of author information is available at the end of the article

Keywords: CE-QUAL-W2, *Planktothrix rubescens*, Drinking water reservoir, Selective withdrawal, Light extinction, Deep chlorophyll maximum (DCM)

Introduction and background

Cyanobacteria can form dense and toxic blooms in lentic waters, which severely threatens the development of aquatic ecosystems and human health [22]. Cyanobacteria blooms can block sunlight and their breakdown consumes oxygen that other organisms need to live [41]. In addition, during the growth period, cyanobacteria often produce cyanotoxins, which are dangerous for water safety to humans, aquatic organisms and farmed animal stocks without remedies to counteract the effects [50]. A global survey indicates that the cyanobacteria blooms are nowadays increasing in magnitude, frequency and duration in freshwater lakes worldwide [17, 20, 21]. These blooms are often directly visible, because they occur at the surface layer and even form scums allowing management authorities to initiate precautionary measures [7]. A different situation arises for subsurface or deep chlorophyll maxima which may also include dense cyanobacteria populations. They are generally less visible and often overlooked [65] though they can be toxic as well and often occur in sensitive water bodies, such as drinking water reservoirs. Phytoplankton in subsurface chlorophyll maxima tradeoff between increasingly limited light supply with depth and access to nutrients from deeper layers [1, 9]. The light penetrating below the mixed layer is critical for the presence and depth of subsurface chlorophyll layers. Hence, the occurrence of subsurface chlorophyll maxima is usually restricted to relatively clear oligo- or mesotrophic lakes and reservoirs [19, 33].

Planktothrix rubescens (hereafter *P. rubescens*) is a cyanobacterium that often forms metalimnetic chlorophyll maxima in deep oligo- or mesotrophic waterbodies, including reservoirs and lakes commonly used for drinking water supply [10]. It is a filamentous cyanobacterium that potentially contains hepatotoxic peptides known as microcystins [13, 32], so its occurrence in drinking water bodies poses a serious human health concern [3]. *P. rubescens* typically grows in a subsurface layer below the epilimnion of stratified waters [17, 45]. Its name derives from the characteristic red colour associated with the pigment phycoerythrin, which enhances photon capture of green-shifted light in deeper water layers [53].

P. rubescens is highly competitive in nutrient-depleted environments [6] and the subsurface light climate is considered to be critical to its growth [49]. It regulates the vertical position in water column by adjusting its density according to ambient light levels [60] to generate buoyancy under low light levels. At higher light levels, by contrast, it accumulates carbohydrates which act as a ballast and reduces buoyancy [63]. Laboratory experiments and field studies have shown that the depth of neutral buoyancy lies in a range of photosynthetically active radiation (PAR) between 0.28 mol m^{-2} d^{-1} and 0.51 mol m^{-2} d^{-1} [62, 64]. After initially being dispersed in the well-mixed water column in spring, *P. rubescens* develops subsurface 'blooms' as stratification strengthens in summer, if the depth of neutral buoyancy is greater than the mixed layer depth [35]. Decreasing ambient light in autumn, followed by deepening of the mixed layer, often causes the subsurface population to be dispersed into the surface mixed layer again, and has occasionally been associated with surface blooms [14, 65].

Previous research has confirmed that increased duration and strength of seasonal stratification, due to projected climate changes [58], could favor the dominance of buoyancy-regulating *P. rubescens* [6, 28]. Finding an effective strategy to control its growth hence receives increasing concern. Despite a series of physical, chemical and biological strategies (including dredging, physical flushing, application of precipitating phosphorus, selective grazing, etc.) in mitigating cyanobacterial blooms [46], most of them merely dealt with surface blooms typical for eutrophic/hypertrophic lakes [18, 34, 55] but neglected subsurface blooms typical for oligo- or mesotrophic lakes (e.g., metalimnetic blooms of *P. rubescens*).

In reservoir management, depth-selective withdrawal—i.e., removing water from a specific outlet height—is an appealing option. It has been used to affect biogeochemical cycling [66] or to control vertical heat exchange [40]. Previous studies have illustrated that selective withdrawal can redistribute the dissolved oxygen in the water column [5], decrease nutrient concentrations [11], and change the dominant algal assemblages [55]. This body of research indicates that selective water withdrawal may also have potential to control *P. rubescens* blooms but this has never been explored so far. For concrete management targets, moreover, detailed recommendations for optimal withdrawal timing, discharge and duration need to be identified. Our research aims at bridging this research gap by a systematic analysis of alternative withdrawal strategies with respect to their effects on *P. rubescens* dynamics.

Besides management measures, also the surrounding environmental factors come into play and light availability appears to be a key factor for *P. rubescens* growth (e.g., [17, 65]. Any changes in colored dissolved organic matter

[75], phytoplankton biomass [72] or non-algal particles [2], will affect the vertical light climate and the dynamics of *P. rubescens* populations. Accordingly, we also included an analysis checking the response of *P. rubescens* dynamics to different light conditions.

In this study, the two-dimensional (2D) water quality model (CE-QUAL-W2) was used to simulate the dynamics of *P. rubescens* in Germany's largest drinking water reservoir, Rappbode Reservoir. Our previous research has confirmed the dominance of *P. rubescens* in the metalimnion of the reservoir in summer [68], and the model CE-QUAL-W2 showed good performance in capturing the spatial and temporal distribution of *P. rubescens* as well as nutrient and oxygen dynamics in the water column [39]. In the current study, several application-oriented scenarios were designed based on the established model, with the aim to address three questions:

(1) Is it possible to influence or control the population of *P. rubescens* by selective water withdrawal?
(2) What is an optimal timing and amount of water for the withdrawal strategy to remove *P. rubescens*?
(3) How does light extinction within the water column affect the population and growth period of *P. rubescens*?

Since the occurrence of *P. rubescens* is a common and increasing problem in stratified lakes and reservoirs worldwide [28, 49, 68], we believe that the importance of this study reaches beyond the case of Rappbode Reservoir, and it provides a strategy that could be considered by scientists, stakeholders and managers working on other reservoirs with similar problems.

Methods

Study site

Rappbode Reservoir (51.74°N, 10.89°E) is located in the Harz Mountains in central Germany (crest elevation at 423.6 m above sea level (masl), Fig. 1). With a maximum water storage of over 100 million m^3, Rappbode Reservoir is the largest drinking water reservoir in the country, providing drinking water for over one million people. The reservoir has a maximum surface area of 395 ha, and a maximum depth of 89 m (28.6 m mean depth) at full storage. It is fed by the tributaries from Hassel and Rappbode pre-reservoirs, and receives water transfers from the Koenigshuette pre-reservoir [30]. The reservoir dam has five outlets for drinking water supply at different elevations (from 360 to 400 masl in 10 m intervals) from which the lowest one (at 360 masl) was used for most of the time, and a deep outlet discharging water into the downstream Wendefurth Reservoir, which is mainly used for flood protection and hydropower production, from 345 masl [38]. The water residence time of the reservoir is approximately 1 year (344–380 days, [56]. Rappbode Reservoir is a dimictic waterbody, which stratifies in summer, partly freezes in winter and fully mixes in spring and autumn [67]. The reservoir ecosystem is currently in a meso/oligotrophic state (TP concentration dropped to 0.027 mg L^{-1} after 1990, see [67]. However, recent studies

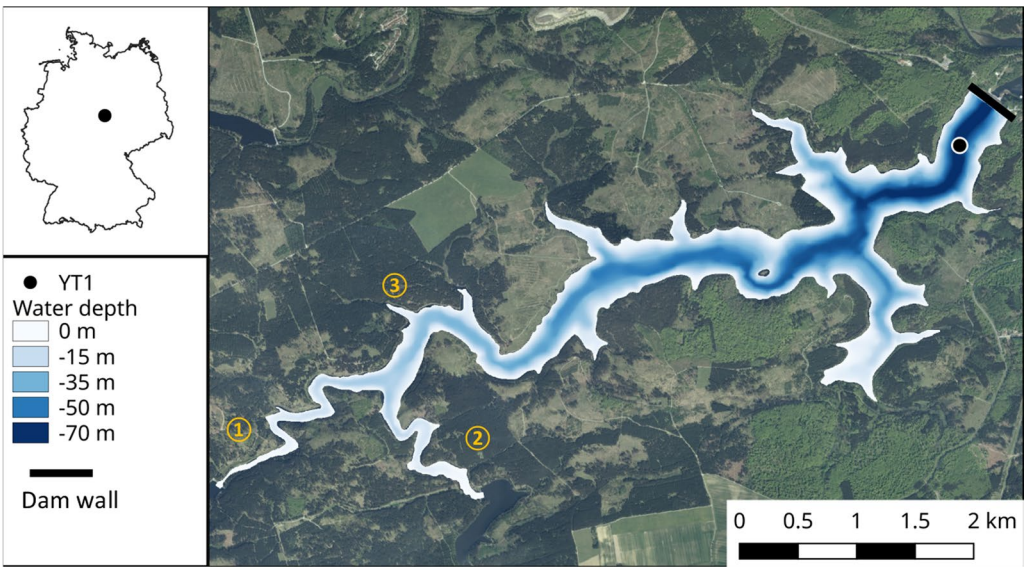

Fig. 1 Map of Germany (top left). The black point indicates the location of Rappbode Reservoir. Bathymetric map of the Rappbode Reservoir (right). The black point shows the sampling location. The yellow number shows the entry of three pre-reservoirs: ① Rappbode, ② Hassel, ③ Koenigshuette

showed that the waterbody experiences regular metalimnetic oxygen minima, which is presumably caused by both pelagic (biological activities of *P. rubescens* in the metalimnion) and benthic (sediment oxygen demand) processes [40, 68].

Water quality model

In this study a two-dimensional water quality model CE-QUAL-W2, version 4.1, was used to simulate the Rappbode Reservoir. CE-QUAL-W2 was launched in 1975 by Edinger and Buchak from the U.S. Army Corps of Engineers. It has been widely used in analyzing thermal structure and eutrophication processes for lakes and reservoirs worldwide (e.g., [5, 24, 29, 47], and its source code is freely available from the official website (https://www.cee.pdx.edu/w2/). As a vertically resolved 2D model, CE-QUAL-W2 is well-suited for simulating waterbodies with a long and narrow shape, which is the case for the Rappbode Reservoir [56].

Model setup and boundary conditions

The model setup was drawn from our previous research in Rappbode Reservoir (see [39] on metalimnetic oxygen dynamics and the physical and ecological sub-models were carefully calibrated by comparisons with observed data. The reservoir basin is divided into 4 branches with 106 horizontal segments and 3976 grid cells, and the vertical spacing for each cell is 1 m. According to the dominating phytoplankton community structure, one specialized cyanobacteria (*P. rubescens*) and a group with physiological parameters linked to diatoms are differentiated. Besides these, nutrients (nitrogen, phosphorus, silicate), detritus components, dissolved oxygen and water temperature were included in the simulation as state variables.

Input boundary conditions

Input data for the model include meteorological conditions, inflow (containing discharge, water temperature, nutrients) and outflow discharge. The meteorological data contain wind speed and direction, shortwave radiation, air temperature, dew point temperature and cloud fraction and most of them were obtained from our monitoring buoy in the reservoir, with missing values filled by measurements from the Harzgerode station of the German Weather Service [37]. The daily inflow and outflow discharges were given by the reservoir authority (Talsperrenbetrieb Sachsen-Anhalt), inflow water temperatures were obtained from a YSI-6200 probe at the pre-reservoirs and Königshütte Reservoir [38]. Inflow nutrients (ammonia, nitrate, silicate, orthophosphate) were biweekly measured by continuous flow photometry (CFA, Skalar, The Netherlands) [16].

Observational data, model specification and calibration

The model was run and calibrated from January 19th to December 31st in 2016, which was covered by high quality observational data for both water temperature and ecological variables. Measurements for the field data were taken close to the dam (see Fig. 1) containing: (1) biweekly profiles of water temperature and dissolved oxygen, measured by a Hydrolab DS5 probe; (2) biweekly profiles of nutrient concentration (including silicate, nitrate, phosphate and ammonia, taken at 10 depths if the reservoir is well-filled), measured by accredited methods following German standards (see [67]; (3) biweekly profiles of phytoplankton concentration (*P. rubescens* and diatoms), measured by a multi-channel fluorescence probe at a vertical resolution of approximately 30 cm (FluoroProbe, bbe moldaenke GmbH). We additionally determined the plankton community structure by microscopic counts at 10 different depths (for more information the reader is referred to Wentzky et al. [68].

Phytoplankton community dynamics in Rappbode Reservoir over the last decade, including conditions at 2016, showed typical and reoccurring succession patterns. A detailed analysis of taxonomic and functional characteristics of the community structure was realized by Wentzky et al. [69] and documented the dominant features: in spring, a strong diatom bloom occurs in the epilimnion with an average chlorophyll concentration around 5 µg L^{-1} [68]. The bloom is terminated in summer, when diatom cells are lost from the euphotic layer by sedimentation. *P. rubescens* is then proliferating in the metalimnion with the average chlorophyll concentration around 4 µg L^{-1}. The winter is regarded as the dormant period, i.e., in which the chlorophyll concentration is very low. Other algal groups besides diatoms and *P. rubescens* play only marginal roles in phytoplankton community dynamics except a group of mixotrophic algae (e.g., *Dinobryon*), but their overall contribution to primary production remained limited due to their partly heterotrophic nutrition.

Finally, note that we could not calibrate ammonia or phosphate, because most measurements in 2016 were below the detection limit (< 0.01 mg L^{-1} for ammonia, < 0.003 mg L^{-1} for phosphate). Details about the model calibration and parameterization are available in the Supplemental Material.

In the reference simulation (Scenario R), CE-QUAL-W2 reproduced observed ecosystem dynamics in Rappbode Reservoir with comparatively high accuracy for water temperature (RMSE = 0.45 °C, $R^2 = 0.99$), dissolved oxygen (RMSE = 0.95 mg L^{-1}, $R^2 = 0.84$), the biomass of diatoms (RMSE = 0.73 µg L^{-1}, $R^2 = 0.55$) and *P. rubescens* (RMSE = 0.65 µg L^{-1}, $R^2 = 0.56$). In addition, the model satisfactorily reproduced the spring

bloom of diatoms, summer bloom of *P. rubescens* and the phenomenon of metalimnetic oxygen minimum in late summer (Fig. 2). The blooming *P. rubescens* manages to persist in the metalimnion by a physiologically mediated buoyancy regulation as described above [64]. We intentionally defined the model for *P. rubescens* without these complex ecophysiological mechanisms, because this would increase the number of parameters and state variables considerably. Instead, our model did not explicitly account for active movements but rather a near-neutral buoyancy and very low sinking velocities. This allows *P. rubescens* in the model to persist at layers, where growth is sufficiently high to compensate for the small losses for this active mobility mechanism. Due to its low light saturation intensity at the maximum photosynthetic rate (8 w m^{-2}) and specific temperature range for its growth (5–18 °C), which are corresponding well with its physiological traits from measurements [23], the population of *P. rubescens* remained restricted to the metalimnion. The same method was applied in Kerimoglu et al. [26] and also on our case well-reproduced the spatio-temporal dynamics of *P. rubescens*. For the general model performance in reproducing other water quality variables in the reservoir, the readers are referred to Mi et al. [39].

We also performed the sensitivity analysis by changing each input parameter by (±5% and ±10%), and calculated the specific sensitivity coefficients (SSC, Additional file 1: Table S3) for the maximum concentration of *P. rubescens* (see supplement material). Despite changes of the maximum concentration under perturbations of parameters, the model always showed a stable reproduction for the key pattern of *P. rubescens* dynamics, particularly with respect to its metalimnetic occurrence indicating high model robustness (see Additional file 1: Fig. S1).

Scenarios

Scenario V: effect of metalimnetic withdrawal volume on the P. rubescens bloom

We established seven scenarios, with different withdrawal volumes (V) to examine the effectiveness of selective water withdrawal on controlling the *P. rubescens* bloom in Rappbode Reservoir (see Table 1). In 2016, *P. rubescens* concentration (given as chlorophyll *a*) increased rapidly at around 11 m depth (i.e., metalimnion) from days 133 to 248 (see Fig. 3). Accordingly, in the V scenarios, we simulated the selective withdrawal during this period at a constant water depth of 11 m. Selective withdrawal water was directed as

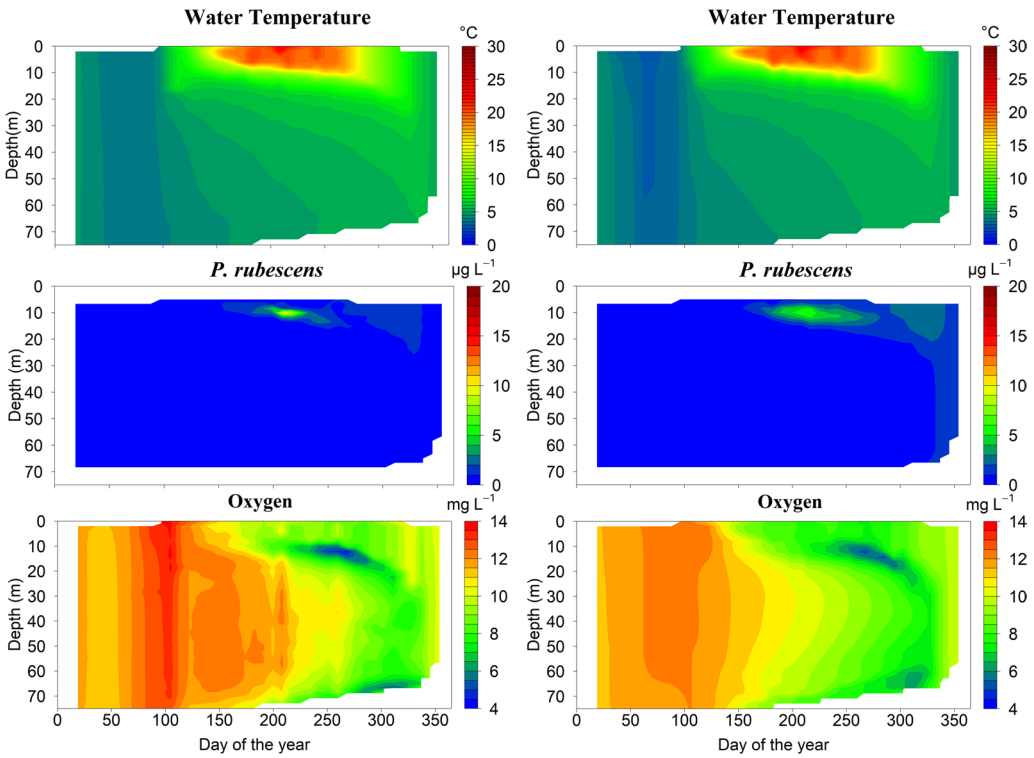

Fig. 2 Observed (left) and simulated (right) results for: water temperature (top), *P. rubescens* concentration (in terms of chlorophyll *a*, middle) and oxygen concentration (bottom) in 2016 in Rappbode Reservoir

Table 1 Overview of factors altered for scenarios *R*, *L*, *V*, and *T*; all other model settings remained identical across all scenarios

	Scenario	Light extinction coefficient (m^{-1})	Metalimnetic withdrawal depth	Metalimnetic withdrawal discharge	Metalimnetic withdrawal timing
	Scenario R	0.45	–	–	–
	Scenario $L_{0.35}$	0.35	–	–	–
	Scenario $L_{0.55}$	0.55	–	–	–
	Scenario $L_{0.65}$	0.65	–	–	–
	Scenario $L_{0.90}$	0.9	–	–	–
	Scenario V_{min}	0.45	11 m below surface	Measurements in 2016	Days 133–248
	Scenario V_1	0.45	11 m below surface	1 m^3 s^{-1}	Days 133–248
	Scenario V_2	0.45	11 m below surface	2 m^3 s^{-1}	Days 133–248
	Scenario V_3	0.45	11 m below surface	3 m^3 s^{-1}	Days 133–248
	Scenario V_4	0.45	11 m below surface	4 m^3 s^{-1}	Days 133–248
	Scenario V_5	0.45	11 m below surface	5 m^3 s^{-1}	Days 133–248
	Scenario V_{max}	0.45	11 m below surface	Maximum in historical measurements[a]	Days 133–248
T_{early}	Scenario T_{133}	0.45	11 m below surface	Maximum in historical measurements[b]	Days 133–156
	Scenario T_{140}	0.45	11 m below surface	Maximum in historical measurements[b]	Days 140–163
	Scenario T_{147}	0.45	11 m below surface	Maximum in historical measurements[b]	Days 147–170
	Scenario T_{154}	0.45	11 m below surface	Maximum in historical measurements[b]	Days 154–177
	Scenario T_{161}	0.45	11 m below surface	Maximum in historical measurements[b]	Days 161–184
T_{bloom}	Scenario T_{168}	0.45	11 m below surface	Maximum in historical measurements[b]	Days 168–191
	Scenario T_{175}	0.45	11 m below surface	Maximum in historical measurements[b]	Days 175–198
	Scenario T_{182}	0.45	11 m below surface	Maximum in historical measurements[b]	Days 182–205
	Scenario T_{189}	0.45	11 m below surface	Maximum in historical measurements[b]	Days 189–212
	Scenario T_{196}	0.45	11 m below surface	Maximum in historical measurements[b]	Days 196–219
T_{late}	Scenario T_{203}	0.45	11 m below surface	Maximum in historical measurements[b]	Days 203–226
	Scenario T_{210}	0.45	11 m below surface	Maximum in historical measurements[b]	Days 210–233
	Scenario T_{217}	0.45	11 m below surface	Maximum in historical measurements[b]	Days 217–240
	Scenario T_{224}	0.45	11 m below surface	Maximum in historical measurements[b]	Days 224–247
	Scenario T_{231}	0.45	11 m below surface	Maximum in historical measurements[b]	Days 231–254

Detailed information of each scenario can be referred to the corresponding paragraph in Model setup and boundary conditions.

[a] Metalimnetic withdrawal discharge in scenario V_{max} is the maximum discharge for each day of the year from 133 to 248, based on long-term measurements (years 1996–2015).

[b] Metalimnetic withdrawal discharge in scenario T is the maximum discharge at each day from 182 to 205, based on long-term measurements

discharge towards Wendefurth reservoir (i.e., downstream release), while the withdrawal for drinking water was still taken in all scenarios from the hypolimnion. This deep raw water extraction is the standard case and preferred mode due to low temperature and turbidity in the location.

In scenario V_{min}, metalimnetic water was withdrawn with the same (downstream) discharge as originally measured during the corresponding period in 2016. Considering the relatively low discharge in this scenario (average 0.66 m^3 s^{-1}), we designed another scenario with the maximum metalimnetic withdrawal discharge. This was defined using the daily maximum discharge from historical measurements, at each specific day, from days 133 to 248 between 1996 and 2015 (scenario V_{max}). In this scenario, the average discharge during the period is 5.43 m^3 s^{-1}, i.e., nearly eight times larger than in V_{min}. To analyze the effect of withdrawal volume on *P. rubescens* in a systematic way, we finally developed five scenarios in which the discharge was increased from 1 to 5 m^3 s^{-1} at intervals of 1 m^3 s^{-1}, during the period mentioned above (days 133–248, scenarios V_1–V_5). We analyzed the results by segmented regression, using the R package "segmented" [43], to elucidate the relationship between metalimnetic withdrawal volume and the maximum *P. rubescens* concentration.

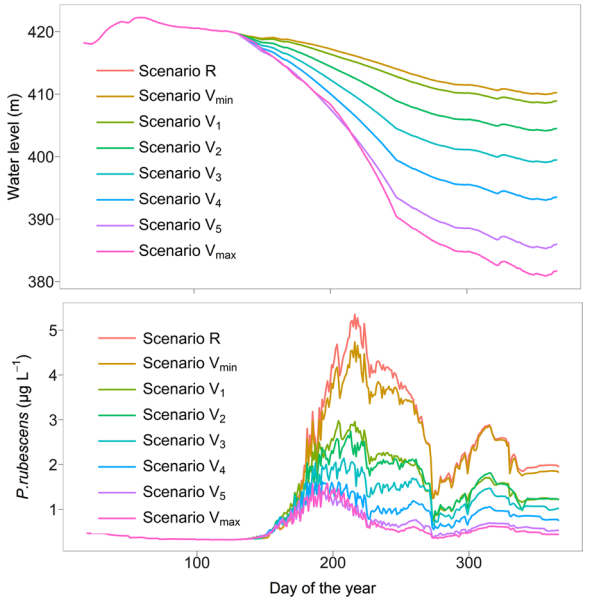

Fig. 3 Water level (top) and concentration of *P. rubescens* (bottom, as chlorophyll *a*) in the metalimnion (i.e., between 10 and 12 m) under scenarios *R* and *V* (see Table 1 for details). Note that in the upper plots, the lines for *R* and V_{min} are plotted on top of each other

Scenario T: effect of metalimnetic withdrawal timing on the P. rubescens bloom

To characterize the time window (T) of selective water withdrawal that most effectively controls *P. rubescens*, we developed 15 sub-scenarios in Scenario T in which metalimnetic withdrawal was applied over a duration of 23 days. We varied the starting time of each period from days 133 to 231 at 1-week intervals (i.e., T133, T140,...T231). We used the maximum daily discharge at each day between days 182 and 205 (years 1996–2015), which represents the midmost of the applied timespans, for defining the withdrawal amounts (Table 1). This ended up in an average discharge of 4.39 m^3 s^{-1} in all T-scenarios, representing 8.7 million m3 and accounts for 9% of the reservoir storage. For making these results tangible and easier to present, we divided them into 3 main groups with the first 5 scenarios as the early group phase (T_{early}), the second group of five as the main bloom phase (T_{bloom}), and the third group as the late bloom phase of decreasing biomass (T_{late}, see also Table 1). At all other times the discharge and withdrawal elevation for the downstream reservoir and the drinking water supply were the same as in the reference simulation (i.e., Scenario R).

We want to emphasize, again, that in scenario V, as well as scenario T a depth-specific water withdrawal was applied and not the existing outlets at the current dam.

Scenario L: effect of the background light condition on P. rubescens growth

In this scenario, we varied the light environment (L) experienced by *P. rubescens*. Photosynthetically active radiation (PAR) at depth z (I_z in mol m^{-2} day^{-1}) was calculated according to the Lambert–Beer law:

$$I_z = (1-\beta)cI_0e^{-\sum_{i=1}^{imax}\varepsilon_i dz_i} \quad (1)$$

where I_0 is the downwelling shortwave radiation at the water surface, c is the fraction of shortwave radiation that is PAR, set as 0.5 based on Kirk [27], $ß$ is albedo, set to 0.1 based on Williams [71], dz_i is the thickness of layer i (always 1 m) and i_{max} is the layer number at depth z, ε_i is the light extinction coefficient at layer i, which consists of the extinction in algal-free water (ε_b) plus light extinction from phytoplankton (specific extinction coefficient for diatoms, ε_{diatom}, and *P. rubescens*, $\varepsilon_{P.rubescens}$):

$$\varepsilon_i = \varepsilon_b + \varepsilon_{diatom}A_{diatom} + \varepsilon_{P.rubescens}A_{P.rubescens} \quad (2)$$

Since the concentration of diatoms, A_{diatom}, and *P. rubescens*, $A_{P.rubescens}$, varies between layers, light extinction is layer-specific.

To illustrate the response of *P. rubescens* to light conditions, we compared results in the reference simulation (i.e., a background light extinction coefficient ε_b of 0.45 m^{-1}, scenario R) with scenarios, where ε_b was either decreased to 0.35 m^{-1}, or increased to 0.55 m^{-1}, 0.65 m^{-1} and 0.9 m^{-1} (scenario $L_{0.35}$, $L_{0.55}$, $L_{0.65}$, $L_{0.90}$, respectively) which represents the realistic range of the light extinction in Rappbode Reservoir (see Additional file 1: Fig. S4 in Mi et al. [39].

Results

Scenario V: effect of metalimnetic withdrawal volume on the P. rubescens bloom

Metalimnetic water withdrawal effectively decreased the *P. rubescens* bloom in Rappbode Reservoir. Although the seasonal distribution of *P. rubescens* in the *V*-scenarios remained similar to that in the reference simulation, its biomass concentrations clearly decreased in scenarios with increasing metalimnetic discharge (Figs. 3, 4). In the reference simulation (i.e., no metalimnetic withdrawal), the average and maximum concentration of *P. rubescens* (all expressed as chlorophyll *a*) in the metalimnion during summer (10–12 m depth, days 180–240) were 4.0 and 6.12 µg L^{-1}, respectively. These values decreased, for example, to 3.5 and 5.5 µg L^{-1} under scenario V_{min} (metalimnetic withdrawal volume of 6.6 million m^3) and further to 1.1 and 1.9 µg L^{-1} under scenario V_{max} (with metalimnetic withdrawal volume of 55.4 million m^3; see Fig. 4). This

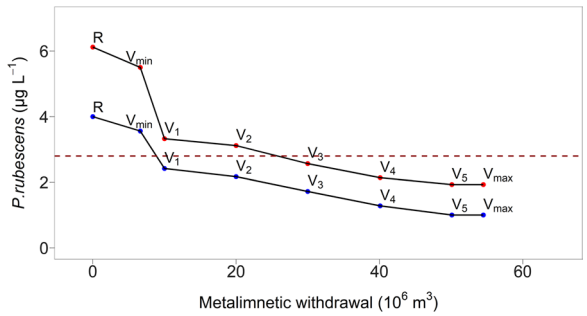

Fig. 4 Average (blue points) and the maximum (red points) concentration of *P. rubescens* (as chlorophyll *a*) in the metalimnion during summer (between 10 and 12 m, from days 180 to 240) under scenario *R* and *V* (see Table 1 for details). The red dashed line indicates the threshold of *P. rubescens* concentration calculated from the WHO report

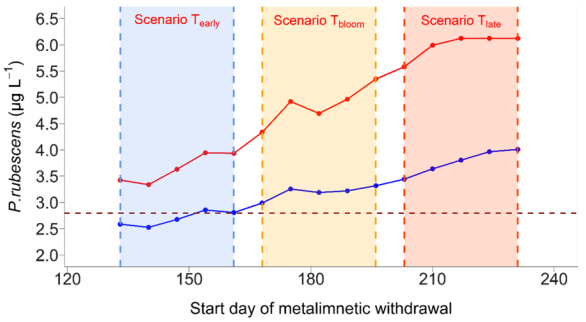

Fig. 5 Average (blue line) and the maximum (red line) *P. rubescens* concentration (as chlorophyll *a*) in the metalimnion during summer (10 to 12 m, from days 180 to 240) under scenario T (see Table 1 for details). The shades show different periods of *P. rubescens* growth used in subsequent scenarios. The red dashed line, in the horizontal direction, indicates the threshold of *P. rubescens* concentration calculated from the WHO report

higher metalimnetic discharge was traded off against decreased water level in the reservoir at the end of the year, from 410 masl under the reference simulation down to 382 masl under scenario V_{max} (Fig. 3). In other words, the costs of removing *P. rubescens* out of the metalimnion arise in terms of water loss.

The relative effect of increasing metalimnetic withdrawal volume on *P. rubescens* was greatest between scenario V_{min} and V_1, while the effect gradually weakened with higher withdrawal volumes (Fig. 4). The results from segmented regression, for withdrawal volume vs *P. rubescens* concentration, indicated a breakpoint at a withdrawal volume of 12.3 million m^3 (i.e., slightly higher than the value under scenario V_1), corresponding to discharge of 1.24 m^3 s^{-1} during the growth period. Below this value the maximum *P. rubescens* concentration decreased by 0.25 µg L^{-1} per million m^3 discharged, while above this value the rate of change was only 0.03 µg L^{-1} decrease per million m^3 discharged, i.e., one order of magnitude lower. Since under scenario V_1 the maximum concentration of *P. rubescens* (i.e., 3.3 µg L^{-1}) already decreased to nearly half of that under the reference simulation (i.e., 6.1 µg L^{-1}) with relatively small change in water withdrawal volume (see Fig. 3), we identified the optimal withdrawal volume to control *P. rubescens* as approximately 10 million m^3 (10% of the reservoir volume), corresponding to discharge of 1 m^3 s^{-1} during the growth period (days 133–248). Based on this optimized scenario, the lowest water level never falls below 408.9 m. This relatively small additional water loss implies that the optimized management only marginally interferes with drinking water security and is, therefore, widely acceptable by reservoir operators (Fig. 3). Under conditions of extreme drought (e.g., in the year 2003), however, the additional water withdrawal may become a concern.

Scenario T: effect of metalimnetic withdrawal timing on the P. rubescens bloom

The main growth phase of *P. rubescens* occurs before it attains the maximum abundance. For the reference simulation, the steady increase of *P. rubescens* began around day 130 and ended on day 215 (Fig. 3) when the biomass peaked (scenario R, Fig. 3). The average specific growth rate in the simulation during this period was 0.032 d^{-1} (10 to 12 m depth), and the maximum was 0.098 d^{-1} on day 177. Thus, to compensate for the growth of *P. rubescens*, an average withdrawal rate equivalent to 0.032 d^{-1} would be required from the metalimnetic water layers. In scenario R, i.e., under the actual reservoir operation conditions that largely follow the snowmelt-dominated hydrology of the catchment, the downstream withdrawal was high only early in the year and relatively low afterwards. If this downstream withdrawal was taken entirely from the metalimnion, specific clearance rates could reach up to 0.1 d^{-1} and, for example, reach an average value of 0.052 $^{-1}$ between days 40 and 90. However, this time window is too early and just before *P. rubescens* can start growing (Additional file 1: Fig. S2). After this period, i.e., during the phase of positive growth after day 130, water withdrawal decreased with the rate below 0.01 d^{-1} (Additional file 1: Fig. S2). Accordingly, effective removal of the cyanobacteria can only be realized, if the selective withdrawal for the downstream river is timed later (as being evaluated in the T-scenarios) to have more overlap with the occurrence of *P. rubescens*.

The results from scenario *T* indicate that the population of *P. rubescens* was most effectively suppressed, if the metalimnetic withdrawal was applied at an early growth stage (i.e., scenarios T_{early}, see Figs. 5, 6). Under these scenarios, the average (maximum) *P. rubescens*

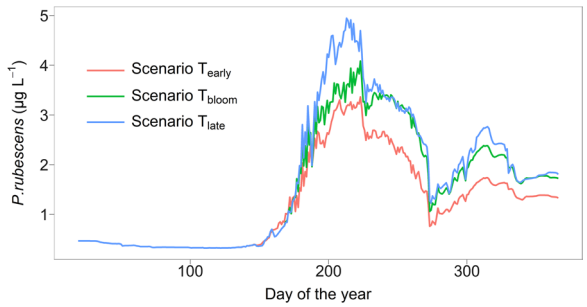

Fig. 6 Concentration of *P. rubescens* (as chlorophyll *a*) in the metalimnion (10 to 12 m) for 2016 under scenario T. Each line indicates the mean result from 5 sub-scenarios included

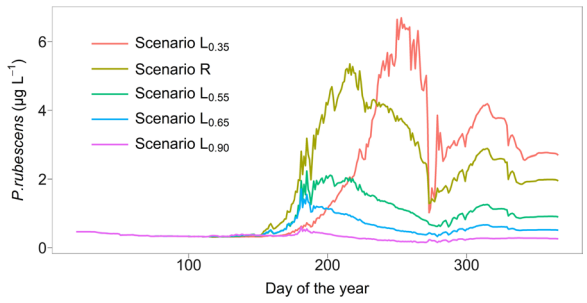

Fig. 7 Concentration of *P. rubescens* (as chlorophyll *a*) in the metalimnion (10 to 12 m for Scenario $L_{0.35}$, R and $L_{0.55}$, and 8 to 10 m for the other two scenarios according to the respective maximum concentration layer of *P. rubscens*) under scenario R and L

concentration at depths from 10 to 12 m always remained below 3.0 µg L^{-1} (4.0 µg L^{-1}), while the value gradually increased to between 3.0 and 3.3 µg L^{-1} (4.3 and 5.3 µg L^{-1}) and further above 3.4 µg L^{-1} (5.5 µg L^{-1}) when water was withdrawn in the blooming (scenarios T_{bloom}) and late bloom stages (scenarios T_{late}). Aside from the standing stock of *P. rubescens*, timing of the maximum concentration as well as spatial patterns were not markedly changed in different T scenarios (Fig. 6).

Scenario L: Effect of the background light condition on *P. rubescens* growth

Growth of *P. rubescens* was gradually suppressed with increased light extinction (Fig. 7). In the reference scenario (background light extinction coefficient $\varepsilon_b = 0.45$ m^{-1}), the maximum concentration in the metalimnion was 5.4 µg L^{-1}. It increased to 6.7 µg L^{-1} under scenario $L_{0.35}$ ($\varepsilon_b = 0.35$ m^{-1}), but decreased to 2.2, 1.7 and 0.7 µg L^{-1} under scenarios $L_{0.55}$, $L_{0.65}$, and $L_{0.90}$. In addition, *P. rubescens* reached maximum concentration later in the year under the lower light extinction. In the reference simulation, the concentration peaked at day 215. This peak was advanced to day 185 under the three scenarios with higher light extinction (Fig. 7) but delayed to day 253 under scenario $L_{0.35}$ with lower light extinction. The later development of the elevated concentrations appeared to be related to longer persistence of diatoms in the metalimnion, with a shift from diatoms to cyanobacteria occurring later in the year (see The role of light intensity in the growth of P. rubescens for Rappbode Reservoir). In addition, low light extinction is prolonging the seasonal time window for *P rubescens* and, therefore, allows to persist longer towards the end of the year. Since in all L scenarios the growth of *P. rubescens* started in the metalimnion around the same time of the year (i.e., around day 125), the results indicate that lower extinction extends the duration of its exponential growth phase. The L-scenarios point to the importance of light conditions for *P rubescens* population dynamics, which is mediated by direct (as a growth-limiting resource) as well as indirect processes (by shifting resource competition within the phytoplankton community).

Discussion

We used a well-established water quality model (CE-QUAL-W2) to demonstrate the influence of water withdrawal strategies and light extinction on the growth of the cyanobacteria *P. rubescens* in Rappbode Reservoir, the largest drinking water reservoir in Germany. Although the occurrence [13], physiology [57] and the toxicity of *P. rubescens* [61] have been well-studied, little is known about active strategies to control blooms of this species. This is a major gap in current research as this highly specialized cyanobacteria can proliferate in nutrient-poor water bodies, which often serve as drinking water sources. Indeed, existing research on cyanobacteria blooms focus largely on surface blooming and scum forming species in eutrophic waters, such as Lake Taihu [21] or recent Lake Erie [48]. However, research has only superficially addressed subsurface blooms like those typically formed by *P. rubescens.* This study advances our knowledge in this respect by adding three novelties: (i) providing an ecosystem model for the prediction of subsurface blooms, (ii) generate concrete reservoir operation strategies to mitigate subsurface blooms in Germany's largest drinking water reservoir, and (iii) identify key environmental factors (light) that affect their occurrence. Needless to say, other environmental factors such as nutrient supply and distribution are also important and require more research in future.

Note that *P. rubescens* has a very low specific chlorophyll *a* content [6] indicating that even the low chlorophyll *a* concentration (like in the Rappbode Reservoir) can correspond to the high biomass producing a high amount of toxic compounds, e.g., microcystins and saxitoxins. Moreover, Rappbode Reservoir is a nutrient-poor

water body (almost oligotrophic) and the formation of such a cyanobacteria population is outstanding and alerting in the context of drinking water provisioning. From the WHO report which comprehensively analyzed the survey data in Germany, the total microcystin content in *P. rubescens* ranges from 2000 to 5000 µg/g dry weight [8]. Based on our measurements the ratio between *P. rubescens* biomass and chlorophyll *a* in terms of mg dry weight/µg chlorophyll *a* is 0.18 [39], so the chlorophyll *a* concentration of 4 µg L^{-1} (i.e., mean value in scenario R) corresponds to the dry weight of 0.72 mg L^{-1} and the total microcystin concentration of 1.44–3.6 µg L^{-1} which is higher than the drinking-water standard from the WHO provisional guideline (1 µg L^{-1}, see [70]). According to the relationship above, to meet the WHO guideline the mean *P. rubescens* concentration (given as chlorophyll *a*) during the growth period should not surpass 2.8 µg L^{-1}. From this perspective, the current *P. rubescens* biomass in Rappbode Reservoir can severely harm the security of drinking water supply and human health. There is a strong need for the reservoir authority, consequently, to optimize the management strategy for suppressing the *P. rubescens* growth in the reservoir. In fact, for Rappbode Reservoir a sampling of microcystin analyses by HPLC in 2021 detected microcystin–LR in the depth of *P. rubescence* occurrence, but the biomass of *P. rubescence* at that time was very low with the microcystin concentration above 0.05 µg/l. Nevertheless, the presence of *P. rubescence* does not necessarily mean that microcystin is produced.

Selective water withdrawal and its influence on growth of *P. rubescens*

Selective water withdrawal is widely used in stratified reservoirs worldwide [12] for optimizing variables that collectively influence water quality (e.g., water temperature, dissolved oxygen concentration, turbidity) within the reservoir or for implementing natural downstream temperature regimes as a component of environmental flows [44]. Various types of infrastructure are adapted to achieve selective withdrawal, such as multi-level offtake towers, temperature-controlled curtains, floating outlets, pivoted pipes or stop-lot gates [52] and each infrastructure component has specific options and restrictions that influence its application. Outlet towers, for example, can only be used to withdraw water at specific depths, while pivoted pipes can be freely moved in the vertical direction to take out water over a continuous depth range. Most previous studies of selective withdrawal have focused on temperature dynamics in the downstream river [66, 74] or within the reservoir [4, 38]. Although the same strategy is in principle also applicable for biogeochemical variables, such as algal biomass, nutrient concentrations and pathogens, such applications had been rarely used or modelled [15, 73]. Our study fills this gap and its practical value should help stakeholders optimize their management strategies and mitigate water quality problems arising from the occurrence of *P. rubescens*.

In fact, infrastructures for depth-specific withdrawal have been established for several German drinking water reservoirs and are currently at the state of planning for Rappbode Reservoir. This points to the fact that managers recognized depth specific withdrawal as a useful instrument. From the management perspective, our specific solution of course includes a prioritization of the water quality in Rappbode Reservoir over the downstream Wendefurth Reservoir, due to the fact that the former is such an important drinking water source, while the latter is just used for hydropower and flood protection. Although cyanobacterial biomass withdrawn by our selective withdrawal regime is a burden for Wendefurth Reservoir, the water quality of Wendefurth is most likely not too much worsening, because it also receives higher amounts of treated wastewater and already by now in an eutrophic state. Note also that lacustrine seston is usually quickly consumed by benthic organisms [54] once it reaches the downstream river (i.e., below Wendefurth Reservoir).

The location of peak *P. rubescens* biomass in the water column corresponds to a physiologically adjustable depth of neutral buoyancy, and may vary in different water bodies [36] and over time due to changing light and nutrient gradients [64]. It is advantageous if the withdrawal facility can precisely follow the depth of *P. rubescens* peak to maximize the potential for its removal. We, therefore, designed withdrawal depth by distance under the water surface, instead of the commonly absolute elevation. This is meaningful, since the outtake depth follows *P. rubescens* peak even in case of water level changes due to hypolimnetic withdrawal of raw water. Moreover, we believe that the selective withdrawal strategy, tested in this study, could remove other harmful or unwanted constituents (e.g., high concentrations of dissolved organic carbon or suspended solids) in reservoirs, as long as its occurrence is restricted to a narrow depth range and the offtake can directly flush the layer containing the constituents out of the water column [55].

Our results also indicate that *P. rubescens* concentrations decreased following the increased water withdrawal volume, but the relative effectiveness in its removal per unit of water withdrawn, is getting weaker at high withdrawal discharge (see Fig. 4). For example, the decrease of *P. rubescens* concentration is much lower from scenario V_2 to V_{max}, than from scenario V_{min} to V_1. This results should be attributed to the changes of stratification intensity under different withdrawal scenarios. Here,

the intensity is represented by buoyancy frequency (N^2) based on the density gradient in water column, which is calculated as [51]

$$N^2 = \frac{g}{\rho}\frac{d\rho}{dz} \tag{3}$$

where g is the acceleration due to gravity, ρ is density and z is depth. The results clearly show that during summer metalimnetic N^2 under scenario V_2 onwards is higher than that under the first two scenarios ($V_{\min}$ and V_1, see Additional file 1: Fig. S3). This indicates high rates of withdrawal increase the stratification intensity and provide a more stable density gradient, which is beneficial to *P. rubescens* growth. Since the average concentration of *P. rubescens* during the blooming period is already below the threshold of 2.8 µg L^{-1} shown above, it is not strongly necessary to continue increase the discharge for its removal from the reservoir. In addition, high withdrawal can be disadvantageous with respect to the loss of water storage. For example, from scenario V_1 to $V_{\max}$, the water level decreased by approximately 5 m for each 10 million m^3 of water withdrawn (Fig. 3). From a stakeholders' perspective, such a dramatic decrease in water level harms water security for drinking water supply, and could have negative influences on water quality due to increases in turbidity and nutrients [76]. Therefore, in most cases there should exist an optimal withdrawal volume for the specific research place (around 10 million m^3 in our case), balancing positive and negative effects.

Withdrawing metalimnetic water at the beginning of *P. rubescens* growth more effectively reduced its concentration in the reservoir than later withdrawals (see Figs. 5, 6). On the one hand, this makes sense as withdrawal is exactly at the time when growth rate is maximal, but on the other hand the accumulated amount of exported biomass should be lower than for a period with later withdrawal. We hypothesize that selective withdrawal—besides the direct effect of biomass export—also induces indirect effects on *P. rubescens* growth by changing the dynamics of soluble reactive phosphorus (SRP) concentration. The supply of phosphorus in the initial *P. rubescens* growth phase appeared to be partly recycled from diatom death. Our simulations indicated that diatoms took up a large proportion of the bioavailable phosphorus in spring before dying, with mineralization then recycling organic phosphorus to its bioavailable inorganic form, again. *P. rubescens* appeared to fill in a niche that exploited this recycled phosphorus. Scenarios with early withdrawal removed a substantial amount of mineralized phosphorus from the system, which was confirmed in our results: SRP concentration at depth 10–12 m, where *P. rubescens* was highest, was always lower in the T_{early} scenarios than in the case of late withdrawal or the reference simulation (up to 2 µg L^{-1} in some cases, see Fig. S4). Since phytoplankton in Rappbode Reservoir is P-limited [67], the reduction in phosphorus concentration in the T_{early} scenarios leads to lower biomass of *P. rubescens* compared with the T_{bloom} and T_{late} scenarios. What's more, the T-scenarios showed that early withdrawal increases the diatom biomass in the surface layers (Additional file 1: Fig. S5) which implies a stronger shading effect from diatoms on the *P. rubescens* residing in the metalimnion, leading to further deterioration of growth conditions for this species.

In the scenarios above, we separately checked the optimal withdrawal volume and timing to suppress the bloom of *P. rubescens*. To further clarify the conclusion, we coupled scenario *V* and scenario *T* together and established another 15 sub-scenarios (scenario VT) in which the optimal discharge (10 million m^3) was evenly withdrawn at the metalimnion during 23 days (corresponding to the daily discharge of 5 m^3 s^{-1}), starting from days 133 to 231 at 1-week intervals. Here, all the other settings are the same as before. Quite close to those from scenario T, the new results suggested that the population of *P. rubescens* was much lower under the strategy applied at its early growth stage than the other two stages (see Additional file 1: Fig. S6), which further verified our previous conclusion and the robustness of the study (i.e., the optimal timing is independent of the withdrawal discharge).

Given its main purpose as a drinking water reservoir, the water storage in Rappbode Reservoir needs to be maintained above a certain volume for water security purposes (10 million m^3 as absolute minimum according to the regulation of the reservoir authority). Since the water level decreases from spring to autumn in Rappbode Reservoir [38], the amount of water potentially available for withdrawal also decreases over the season. The selective withdrawal strategy should, therefore, remain within a "safe operating space" (see Fig. 8) that allows substantial control of *Planktothrix* biomass on the one hand, and guarantees adequate water storage on the other hand.

The role of light intensity in the growth of *P. rubescens* for Rappbode Reservoir

Light intensity is a key factor influencing algal growth in aquatic systems, particularly for subsurface populations that are strongly affected by light extinction within the surface waters [28]. In the metalimnion, PAR from spring to autumn exceeded 0.5 mol m^{-2} day^{-1} and was up to 1.5 mol m^{-2} day^{-1} under clear-water conditions (scenario $L_{0.35}$). In comparison, PAR ranged from 0.1 to 0.5 mol m^{-2} day^{-1} in the reference simulation (ε_b= 0.45 m^{-1}), and remained below 0.2 mol m^{-2} day^{-1} for $\varepsilon_b \geq 0.55$ m^{-1} (see Additional file 1: Fig. S7). In our algal growth model, saturating light intensities are

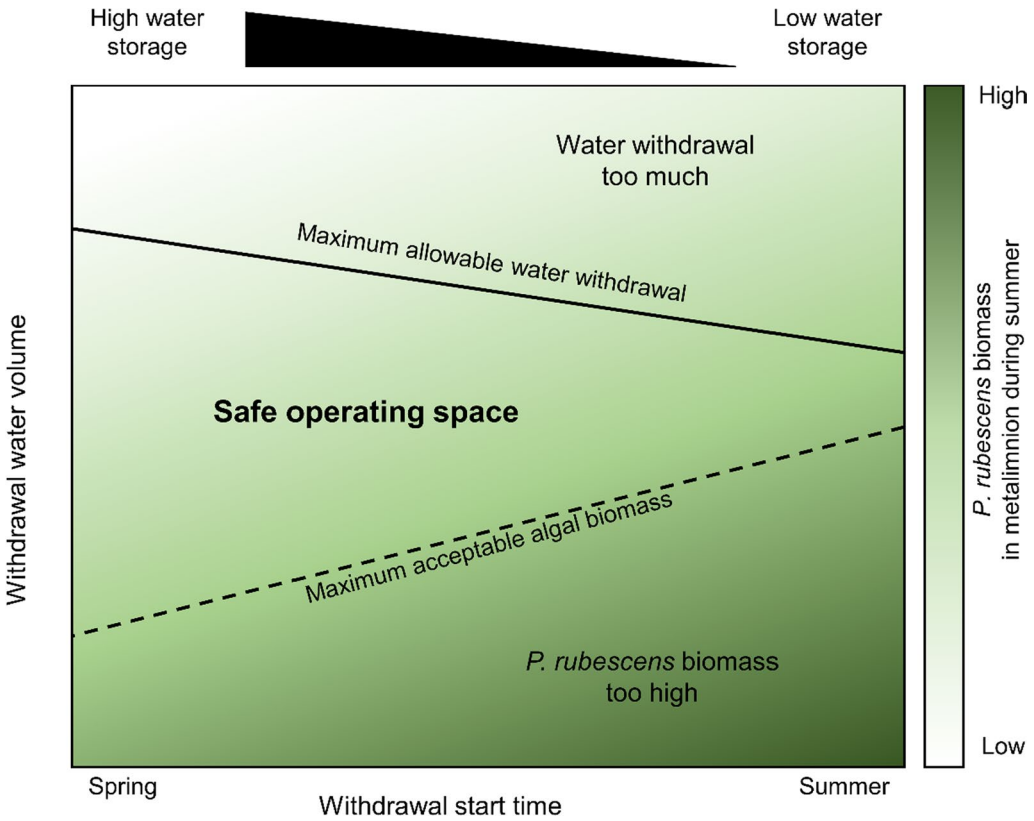

Fig. 8 Conceptual diagram showing the pattern of maximum biomass of *P. rubescens* in the metalimnion of Rappbode Reservoir in summer, under different combinations of withdrawal water volume and withdrawal start time. The pattern is generated from the scenario analysis, which indicates that the phytoplankton biomass would be lower with higher withdrawal volumes and earlier withdrawal (given as color scale, i.e., decreasing towards the upper left corner). The solid line is the maximum withdrawal water volume that allows adequate water storage in the reservoir. The maximum allowable water withdrawal decreases over the season, because the stored water volume declines from spring to summer. The phytoplankton biomass threshold (dashed line) is a critical upper level of *P. rubescens* that can prevent the subsequent development of high concentrations. It increases over the season, since earlier metalimnetic withdrawal can more effectively suppress *P. rubescens* growth compared to the later withdrawal. Between the two lines is the safe operating space as a tradeoff between mitigating harmful cyanobacteria blooms and maintaining water resources

14 mol m^{-2} day^{-1} and 3.2 mol m^{-2} day^{-1} for diatoms and *P. rubescens*, respectively (see [39], indicating substantial light limitation, especially for diatoms, in the metalimnion. Interestingly, since diatoms undergo rapid development in spring (i.e., before the growth of *P. rubescens*) and monopolize nutrients in their biomass [68], scenario $L_{0.35}$ allowed a longer metalimnetic persistence of diatoms (see Additional file 1: Fig. S8), which in turn delayed the growth and occurrence of *P. rubescens* (see Additional file 1: Fig. 7). Again, this points to the importance of indirect effects among phytoplankton groups and a proper representation of community dynamics and competition among phytoplankton groups is required to capture the dynamics at a species level.

Current climate forecasts indicate that due to global warming, air temperature for the study region may increase substantially in this century [40], which will intensify stratification duration and stability potentially supporting the dominance of *P. rubescens* in lakes and reservoirs [28]. Our study suggests that decreasing light intensity in the metalimnion may offset the supportive effects of warming on the *P. rubescens* growth. A number of studies have reported increasing DOC concentrations (i.e., brownification, see Kritzberg et al. [31] in surface waters. This brownification, which is observable at continental scales [42], is coming along with higher light extinction that is interfering with primary production by reducing light availability [25]. Light conditions in the metalimnion are strongly affected by brownification and rising DOC concentrations can effectively shrink or even close the ecological niche for *P. rubescens*. Several drivers can lead to the brownification including changes in climate conditions and land cover, and reduction in

atmospheric acid deposition. Faster flushing rates due to increasing precipitation, for example, restrain DOC sedimentation which leads to elevated DOC. To get a better quantitative understanding about the role of brownification for *P. rubescens* dynamics, further model applications should take these processes into account and deliver useful information for the reservoir operators.

Limitations and future work

The water quality model used in this research systematically elucidates the influence of two important driving factors (i.e., metalimnetic water withdrawal and background light conditions) on *P. rubescens* growth in Rappbode Reservoir. To extend the current study, our model can be used as a template to assess the possibility to also control other harmful cyanobacteria by selective withdrawal, e.g., species associated with surface blooms. For achieving this goal, further model development may be required, e.g., to include other algal groups and new features like vertical migration of phytoplankton cells associated with buoyancy control.

In addition, although metalimnetic water withdrawal can effectively suppress *P. rubescens* growth, the water that is withdrawn could potentially release high levels of cyanobacteria into downstream ecosystems. As indicated by Teurlincx et al. [59], ecological functioning of inland waters can only be comprehensively understood if we take their connections with upstream catchments and downstream receiving waters into account. Accordingly, for future studies, it is recommended to combine upstream catchment models with lake models, as well as models of downstream ecosystems, to upscale the research from local to regional perspective and develop system-level management strategies.

Conclusions

In this work, we applied a well-established water quality model (CE-QUAL-W2) to illustrate the effect of water withdrawal strategies and light extinction on the growth of the cyanobacteria *P. rubescens* in Rappbode Reservoir, Germany's largest drinking water reservoir. The results showed that the selective withdrawal strategy is an effective way to reduce the biomass of *P. rubescens* in the reservoir. Through a scenario analysis we identified the optimal withdrawal volume to suppress the *P. rubescens* bloom as 10 million m^3 (around 10% of the reservoir volume) and were also able to determine an optimal seasonal time window for applying the strategy. The biomass of *P. rubescens* is most effectively suppressed when the metalimnetic withdrawal is applied at an early growth stage (i.e., days 133–161). In addition, underwater light conditions were identified as an important factor for the growth of *P. rubescens* and any increase in light extinction led to lower biomass and shorter duration of its blooms. *P. rubescens* almost disappeared when the extinction coefficient exceeded 0.55 m^{-1}. Considering the widespread occurrence of *P. rubescens* in stratified lakes and reservoirs worldwide, we believe the importance of our research extends beyond the case of Rappbode Reservoir and the results will be helpful to scientists and water managers working on strategies for other water bodies to deal with the bloom of this harmful cyanobacteria.

Abbreviations

2D: Two dimensional; *P. rubescens*: *Planktothrix rubescens*; SRP: Soluble reactive phosphorus; PAR: Photosynthetically active radiation.

Supplementary Information

The online version contains supplementary material available at https://doi.org/10.1186/s12302-022-00683-3.

Additional file 1: Fig. S1. Cumulative frequency for the occurrence time of the maximum *P. rubescens* concentration, based on the simulation results from the sensitivity test scenarios. The vertical dashed line shows the time under the reference simulation (i.e., day of 214). **Fig. S2.** Comparison of net specific growth rates of *P. rubescens* in the reference scenario (scenario R), averaged over the depth layer from 10 to 12 m, with the specific water withdrawal rates from the same water layer. The dashed line indicates the rate of 0. **Fig. S3.** Average buoyancy frequency in the metalimnion (10–12 m, from days 180 to 240) under scenario R and V. **Fig. S4.** Difference in SRP concentration between the reference scenario and scenario T, in the metalimnion during summer (i.e., 10–12 m, from days 180 to 240). The horizontal axis shows the start day of the metalimnetic withdrawal, and vertical axis shows the difference of SRP between the reference scenario and the respective T-scenario (e.g., the first boxplot shows the results of scenario R-scenario T_{133}). The dashed line indicates the value of 0. **Fig. S5.** Vertically averaged concentration of diatoms (as chlorophyll *a*) during summer (days 180–240) for 2016 under scenario T. Each line indicates the mean result from 5 sub-scenarios included. **Fig. S6.** The same as Fig. 5, but under scenario VT. **Fig. S7**. Average photosynthetically active radiation (PAR) in the metalimnion under scenario R and L as outlined in Table 1. **Fig. S8.** Average concentration of diatoms in the metalimnion under scenario R and L as outlined in Table 1. **Table S1.** Values of *a priori* determined parameters including references. **Table S2.** The applied minimum and maximum values as well as their intervals for the calibrated parameters. **Table S3.** Specific sensitivity coefficients (SSC) for the maximum concentration of *P. Rubescens* (absolute values higher than 1 were highlighted by red color).

Acknowledgements

We are grateful to the reservoir authority of the Rappbode Reservoir (Talsperrenbetrieb Sachsen-Anhalt) for providing data.

Author contributions

CM conducted the CE-QUAL-W2 modeling, with the help from DPH and KR. CM, MAF, TS and KR designed research, analyzed data and wrote the manuscript. XK, BB, YL and JD reviewed, edited and proofread the manuscript. All authors read and approved the final manuscript.

Funding

Open Access funding enabled and organized by Projekt DEAL. This project was funded within the Australia–Germany Joint Research Co-operation Scheme by the DAAD—(German Academic Exchange Service) and Universities Australia (project CYANOMOD), the newMOM-project supported by the German Science Foundation under grant DFG RI2040/4-1, the National Natural Science Foundation of China (42107060) and Xingliao Talents Plan (XLYC2002054). Xiangzhen Kong is supported by a postdoctoral fellowship

from the Alexander von Humboldt Foundation in Germany. The reservoir monitoring infrastructure was financially supported by TERENO (TERrestrial ENvironmental Observatories) funded by the Helmholtz Association and the Federal Ministry of Education and Research (BMBF).

Availability of data and materials
The source code of the model CE-QUAL-W2 can be freely downloaded at http://cee.pdx.edu/w2/. All the data sets that support the findings of this study are available from the corresponding author upon reasonable request.

Declarations

Ethics approval and consent to participate
Not applicable.

Consent for publication
Not applicable.

Competing interests
The authors declare that they have no conflict of interest.

Author details
[1]Department of Lake Research, Helmholtz Centre for Environmental Research, Magdeburg, Germany. [2]College of Water Conservancy, Shenyang Agricultural University, Shenyang, China. [3]Australian Rivers Institute, Griffith University, Brisbane, QLD, Australia. [4]Department of Microbial Ecology, German Federal Institute of Hydrology, Koblenz, Germany. [5]State Key Laboratory of Lake Science and Environment, Nanjing Institute of Geography and Limnology, Chinese Academy of Sciences, Nanjing, China. [6]Key Laboratory of Integrated Regulation and Resources Development On Shallow Lakes, Ministry of Education, College of Environment, Hohai University, Nanjing, China. [7]Fernwasserversorgung Elbaue-Ostharz GmbH, Naundorfer Straße 46, 04860 Torgau, Germany.

Received: 13 June 2022 Accepted: 2 October 2022
Published online: 15 October 2022

References

1. Abbott MR, Denman KL, Powell TM, Richerson PJ, Richards RC, Goldman CR (1984) Mixing and the dynamics of the deep chlorophyll maximum in Lake Tahoe 1. Limnol Oceanogr 29:862–878
2. Abdelrhman MA (2016) Modeling water clarity and light quality in oceans. J Marine Sci Eng 4:80
3. Bogialli S, Nigro di Gregorio F, Lucentini L, Ferretti E, Ottaviani M, Ungaro N, Abis PP, Cannarozzi de Grazia M (2013) Management of a toxic cyanobacterium bloom (Planktothrix rubescens) affecting an Italian drinking water basin: a case study. Environ Sci Technol 47:574–583
4. Çalışkan A, Elçi Ş (2009) Effects of selective withdrawal on hydrodynamics of a stratified reservoir. Water Resour Manag 23:1257–1273
5. Carr MK, Sadeghian A, Lindenschmidt K-E, Rinke K, Morales-Marin L (2019) Impacts of varying dam outflow elevations on water temperature, dissolved oxygen, and nutrient distributions in a large prairie reservoir. Environ Eng Sci. https://doi.org/10.1089/ees.2019.0146
6. Carraro E, Guyennon N, Hamilton D, Valsecchi L, Manfredi EC, Viviano G, Salerno F, Tartari G, Copetti D (2012) Coupling high-resolution measurements to a three-dimensional lake model to assess the spatial and temporal dynamics of the cyanobacterium Planktothrix rubescens in a medium-sized lake. In: Salmaso N, Naselli-Flores L, Cerasino L, Flaim G, Tolotti M, Padisák J (eds) Phytoplankton responses to human impacts at different scales. Springer, Hydrobiologia, pp 77–95
7. Chorus I, Falconer IR, Salas HJ, Bartram J (2000) Health risks caused by freshwater cyanobacteria in recreational waters. J Toxicol Environ Health Part B 3:323–347
8. Chorus I, Welker M (2021) Toxic cyanobacteria in water: a guide to their public health consequences, monitoring and management. Taylor and Francis, London
9. Cullen JJ (2015) Subsurface chlorophyll maximum layers: enduring enigma or mystery solved? Ann Rev Mar Sci. https://doi.org/10.1146/annurev-marine-010213-135111
10. D'Alelio D, Gandolfi A, Boscaini A, Flaim G, Tolotti M, Salmaso N (2011) Planktothrix populations in subalpine lakes: selection for strains with strong gas vesicles as a function of lake depth, morphometry and circulation. Freshw Biol 56:1481–1493
11. Dehbalaei FN, Javan M (2018) Assessment of selective withdrawal and inflow control on the hydrodynamics and water quality of ilam reservoir. Water Environ Res 90:307–321. https://doi.org/10.2175/106143017x15131012152834
12. Deng Y, Tuo Y, Li J, Li K, Li R (2011) Spatial-temporal effects of temperature control device of stoplog intake for Jinping i hydropower station. Sci China Technol Sci 54:83–88
13. Ernst B, Hoeger SJ, O'Brien E, Dietrich DR (2009) Abundance and toxicity of Planktothrix rubescens in the pre-alpine lake ammersee Germany. Harmful Algae 8:329–342
14. Fee EJ (1976) The vertical and seasonal distribution of chlorophyll in lakes of the experimental lakes area, northwestern ontario: implications for primary production estimates. Limnol Oceanogr 21:767–783
15. Feldbauer J, Kneis D, Hegewald T, Berendonk TU, Petzoldt T (2020) Managing climate change in drinking water reservoirs: potentials and limitations of dynamic withdrawal strategies. Environ Sci Eur 32:48. https://doi.org/10.1186/s12302-020-00324-7
16. Friese K, Schultze M, Boehrer B, Büttner O, Herzsprung P, Koschorreck M, Kuehn B, Rönicke H, Wendt-Potthoff K, Wollschläger U (2014) Ecological response of two hydro–morphological similar pre-dams to contrasting land-use in the rappbode reservoir system (Germany). Int Rev Hydrobiol 99:335–349
17. Gallina N, Beniston M, Jacquet S (2017) Estimating future cyanobacterial occurrence and importance in lakes: a case study with Planktothrix rubescens in Lake Geneva. Aquat Sci 79:249–263. https://doi.org/10.1007/s00027-016-0494-z
18. Gu P, Zhang G, Luo X, Xu L, Zhang W, Li Q, Sun Y, Zheng Z (2021) Effects of different fluid fields on the formation of cyanobacterial blooms. Chemosphere. https://doi.org/10.1016/j.chemosphere.2021.131219
19. Hamilton DP, O'Brien KR, Burford MA, Brookes JD, McBride CG (2010) Vertical distributions of chlorophyll in deep, warm monomictic lakes. Aquat Sci 72:295–307
20. Ho JC, Michalak AM, Pahlevan N (2019) Widespread global increase in intense lake phytoplankton blooms since the 1980s. Nature 574:667–670
21. Huang J, Zhang Y, Arhonditsis GB, Gao J, Chen Q, Peng J (2020) The magnitude and drivers of harmful algal blooms in China's lakes and reservoirs: a national–scale characterization. Water Res 181:115902
22. Huisman J, Codd GA, Paerl HW, Ibelings BW, Verspagen JMH, Visser PM (2018) Cyanobacterial blooms. Nat Rev Microbiol 16:471–483. https://doi.org/10.1038/s41579-018-0040-1
23. Jacquet S, Kerimoglu O, Rimet F, Paolini G, Anneville O (2014) Cyanobacterial bloom termination: the disappearance of Planktothrix rubescens from Lake Bourget (France) after restoration. Freshw Biol 59:2472–2487
24. Jin J, Wells SA, Liu D, Yang G, Zhu S, Ma J, Yang Z (2019) Effects of water level fluctuation on thermal stratification in a typical tributary bay of three gorges reservoir China,. PeerJ 7:e6925. https://doi.org/10.7717/peerj.6925
25. Karlsson J, Byström P, Ask J, Ask P, Persson L, Jansson M (2009) Light limitation of nutrient-poor lake ecosystems. Nature 460:506–509
26. Kerimoglu O, Jacquet S, Vinçon-Leite B, Lemaire BJ, Rimet F, Soulignac F, Trévisan D, Anneville O (2017) Modelling the plankton groups of the deep, peri-alpine Lake Bourget. Ecol Model 359:415–433
27. Kirk JT (1994) Light and photosynthesis in aquatic ecosystems. Cambridge University Press, Cambridge
28. Knapp D, Fernández Castro B, Marty D, Loher E, Köster O, Wüest A, Posch T (2021) The red harmful plague in times of climate change: blooms of the cyanobacterium planktothrix rubescens triggered by stratification dynamics and irradiance. Front Microbiol. https://doi.org/10.3389/fmicb.2021.705914
29. Kobler UG, Wüest A, Schmid M (2018) Effects of lake-reservoir pumped-storage operations on temperature and water quality. Sustainability 10:1968. https://doi.org/10.3390/su10061968
30. Kong X, Seewald M, Dadi T, Friese K, Mi C, Boehrer B, Schultze M, Rinke K, Shatwell T (2021) Unravelling winter diatom blooms in temperate

lakes using high frequency data and ecological modeling. Water Res 190:116681
31. Kritzberg ES, Hasselquist EM, Škerlep M, Löfgren S, Olsson O, Stadmark J, Valinia S, Hansson L-A, Laudon H (2020) Browning of freshwaters: consequences to ecosystem services, underlying drivers, and potential mitigation measures. Ambio 49:375–390. https://doi.org/10.1007/s13280-019-01227-5
32. Kurmayer R, Gumpenberger M (2006) Diversity of microcystin genotypes among populations of the filamentous cyanobacteria Planktothrix rubescens and Planktothrix agardhii. Mol Ecol 15:3849–3861
33. Leach TH, Beisner BE, Carey CC, Pernica P, Rose KC, Huot Y, Brentrup JA, Domaizon I, Grossart HP, Ibelings BW (2018) Patterns and drivers of deep chlorophyll maxima structure in 100 lakes: the relative importance of light and thermal stratification. Limnol Oceanogr 63:628–646
34. Lewis WM Jr, Wurtsbaugh WA, Paerl HW (2011) Rationale for control of anthropogenic nitrogen and phosphorus to reduce eutrophication of inland waters. Environ Sci Technol 45:10300–10305
35. Lürling M, Mucci M, Waajen G (2020) Removal of positively buoyant planktothrix rubescens in lake restoration. Toxins 12:700
36. Maltese A, Capodici F, Ciraolo G, La Loggia G, Granata A, Corbari C (2012) Planktothrix rubescens in freshwater reservoirs: remote sensing potentiality for mapping cell density. In: Neale CMU, Maltese A (eds) Remote Sensing for Agriculture Ecosystems and Hydrology XIV. SPIE, Bellingham
37. Mi C, Frassl MA, Boehrer B, Rinke K (2018) Episodic wind events induce persistent shifts in the thermal stratification of a reservoir (Rappbode Reservoir, Germany). Int Rev Hydrobiol 103:71–82
38. Mi C, Sadeghian A, Lindenschmidt K-E, Rinke K (2019) Variable withdrawal elevations as a management tool to counter the effects of climate warming in Germany's largest drinking water reservoir. Environ Sci Eur 31:19
39. Mi C, Shatwell T, Ma J, Wentzky VC, Boehrer B, Xu Y, Rinke K (2020) The formation of a metalimnetic oxygen minimum exemplifies how ecosystem dynamics shape biogeochemical processes: a modelling study. Water Res. https://doi.org/10.1016/j.watres.2020.115701
40. Mi C, Shatwell T, Ma J, Xu Y, Su F, Rinke K (2020) Ensemble warming projections in Germany's largest drinking water reservoir and potential adaptation strategies. Sci Total Environ. https://doi.org/10.1016/j.scitotenv.2020.141366
41. Mishra S, Stumpf RP, Schaeffer BA, Werdell PJ, Loftin KA, Meredith A (2019) Measurement of cyanobacterial bloom magnitude using satellite remote sensing. Sci Rep 9:18310. https://doi.org/10.1038/s41598-019-54453-y
42. Monteith DT, Stoddard JL, Evans CD, de Wit HA, Forsius M, Høgåsen T, Wilander A, Skjelkvåle BL, Jeffries DS, Vuorenmaa J, Keller B, Kopácek J, Vesely J (2007) Dissolved organic carbon trends resulting from changes in atmospheric deposition chemistry. Nature 450:537–540. https://doi.org/10.1038/nature06316
43. Muggeo VM, Muggeo MVM (2017) Package 'segmented.' Biometrika 58:516
44. Olden JD, Naiman RJ (2010) Incorporating thermal regimes into environmental flows assessments: modifying dam operations to restore freshwater ecosystem integrity. Freshw Biol 55:86–107
45. Padisák J, Crossetti LO, Naselli-Flores L (2009) Use and misuse in the application of the phytoplankton functional classification: a critical review with updates. Hydrobiologia 621:1–19
46. Paerl HW (2018) Mitigating toxic planktonic cyanobacterial blooms in aquatic ecosystems facing increasing anthropogenic and climatic pressures. Toxins 10:76
47. Park H, Chung S, Cho E, Lim K (2018) Impact of climate change on the persistent turbidity issue of a large dam reservoir in the temperate monsoon region. Clim Change. https://doi.org/10.1007/s10584-018-2322-z
48. Pirasteh S, Mollaee S, Fatholahi SN, Li J (2020) Estimation of phytoplankton chlorophyll-a concentrations in the western basin of lake erie using sentinel-2 and sentinel-3 data. CaJRS 46:585–602
49. Posch T, Koster O, Salcher MM, Pernthaler J (2012) Harmful filamentous cyanobacteria favoured by reduced water turnover with lake warming. Nat Clim Chang 2:809–813. https://doi.org/10.1038/nclimate1581
50. Rastogi RP, Madamwar D, Incharoensakdi A (2015) Bloom dynamics of cyanobacteria and their toxins: environmental health impacts and mitigation strategies. Front Microbiol. https://doi.org/10.3389/fmicb.2015.01254
51. Read JS, Hamilton DP, Jones ID, Muraoka K, Winslow LA, Kroiss R, Wu CH, Gaiser E (2011) Derivation of lake mixing and stratification indices from high-resolution lake buoy data. Environ Model Softw 26:1325–1336. https://doi.org/10.1016/j.envsoft.2011.05.006
52. Ren W, Wei J, Xie Q, Miao B, Wang L (2020) Experimental and numerical investigations of hydraulics in water intake with stop-log gate. Water 12:1788
53. Reynolds CS (2006) The ecology of phytoplankton. Cambridge University Press, Cambridge
54. Richardson JS, Mackay RJ (1991) Lake outlets and the distribution of filter feeders: an assessment of hypotheses. Oikos. https://doi.org/10.2307/3545503
55. Rigosi A, Rueda FJ (2012) Hydraulic control of short-term successional changes in the phytoplankton assemblage in stratified reservoirs. Ecol Eng 44:216–226. https://doi.org/10.1016/j.ecoleng.2012.04.012
56. Rinke K, Kuehn B, Bocaniov S, Wendt-Potthoff K, Buttner O, Tittel J, Schultze M, Herzsprung P, Ronicke H, Rink K, Rinke K, Dietze M, Matthes M, Paul L, Friese K (2013) Reservoirs as sentinels of catchments: the Rappbode Reservoir observatory (Harz Mountains, Germany). Environ Earth Sci 69:523–536. https://doi.org/10.1007/s12665-013-2464-2
57. Selmeczy GB, Tapolczai K, Casper P, Krienitz L, Padisák J (2016) Spatial- and niche segregation of DCM-forming cyanobacteria in Lake Stechlin (Germany). Hydrobiologia 764:229–240
58. Shatwell T, Thiery W, Kirillin G (2019) Future projections of temperature and mixing regime of European temperate lakes. Hydrol Earth Syst Sci 23:1533–1551
59. Teurlincx S, van Wijk D, Mooij WM, Kuiper JJ, Huttunen I, Brederveld RJ, Chang M, Janse JH, Woodward B, Hu F (2019) A perspective on water quality in connected systems: modelling feedback between upstream and downstream transport and local ecological processes. Curr Opin Environ Sustain 40:21–29
60. Trbojević I, Blagojević A, Kostić D, Marjanović P, Krizmanić J, Popović S, Simić GS (2019) Periphyton development during summer stratification in the presence of a metalimnetic bloom of Planktothrix rubescens. Limnologica 78:125709
61. Viaggiu E, Melchiorre S, Volpi F, Di Corcia A, Mancini R, Garibaldi L, Crichigno G, Bruno M (2004) Anatoxin-a toxin in the cyanobacterium Planktothrix rubescens from a fishing pond in northern Italy. Environ Toxicol 19:191–197
62. Walsby A, AE W, HC U (1983) Buoyancy changes of a red coloured Oscillatoria agardhii in Lake Gjersjoen. Norway
63. Walsby A, Schanz F (2002) Light-dependent growth rate determines changes in the population of Planktothrix rubescens over the annual cycle in Lake Zürich. Switzerland, New Phytol 154:671–687
64. Walsby AE, Ng G, Dunn C, Davis PA (2004) Comparison of the depth where Planktothrix rubescens stratifies and the depth where the daily insolation supports its neutral buoyancy. New Phytol 162:133–145
65. Walsby AE, Jüttner F (2006) The uptake of amino acids by the cyanobacterium Planktothrix rubescens is stimulated by light at low irradiances. Fems Microbiol Ecol 58:14–22
66. Weber M, Rinke K, Hipsey M, Boehrer B (2017) Optimizing withdrawal from drinking water reservoirs to reduce downstream temperature pollution and reservoir hypoxia. J Environ Manage 197:96–105
67. Wentzky VC, Tittel J, Jäger CG, Rinke K (2018) Mechanisms preventing a decrease in phytoplankton biomass after phosphorus reductions in a German drinking water reservoir—results from more than 50 years of observation. Freshw Biol 63:1063–1076. https://doi.org/10.1111/fwb.13116
68. Wentzky VC, Frassl MA, Rinke K, Boehrer B (2019) Metalimnetic oxygen minimum and the presence of Planktothrix rubescens in a low-nutrient drinking water reservoir. Water Res. https://doi.org/10.1016/j.watres.2018.10.047
69. Wentzky VC, Tittel J, Jäger CG, Bruggeman J, Rinke K (2020) Seasonal succession of functional traits in phytoplankton communities and their interaction with trophic state. J Ecol 108:1649–1663. https://doi.org/10.1111/1365-2745.13395
70. WHO (2004) Back ground document or development of WHO guidelines for drinking-water quality. Fax 41:791
71. Williams DT (1981) Determination of light extinction coefficients in lakes and reservoirs. American Society of Civil Engineers, Proceeding of the Symposium on Surface Water Impoundments, pp 1329–1335

72. Williams GN, Larouche P, Dogliotti AI, Latorre MP (2018) Light absorption by phytoplankton, non-algal particles, and dissolved organic matter in san jorge gulf in summer. Oceanography 31:40–49
73. Zhang M, Lin Q-Q, Xiao L-J, Wang S, Qian X, Han B-P (2013) Effect of intensive epilimnetic withdrawal on phytoplankton community in a (sub) tropical deep reservoir. J Limnol 72:e35–e35
74. Zheng T, Sun S, Liu H, Xia Q, Zong Q (2017) Optimal control of reservoir release temperature through selective withdrawal intake at hydropower dam. Water Sci Tech Water Supp 17:279–299
75. Zhou Y, Davidson TA, Yao X, Zhang Y, Jeppesen E, de Souza JG, Wu H, Shi K, Qin B (2018) How autochthonous dissolved organic matter responds to eutrophication and climate warming: evidence from a cross-continental data analysis and experiments. Earth-sci Rev 185:928–937
76. Zohary T, Ostrovsky I (2011) Ecological impacts of excessive water level fluctuations in stratified freshwater lakes. Inland Waters 1:47–59

Publisher's Note